IOVS Papers in Press. Published on July 21, 2011 as Manuscript iovs.11-7762

Photoreceptor Structure and Function in Patients with Congenital Achromatopsia

Mohamed A. Genead, MD, [1, 2] Gerald A. Fishman, MD, [1, 2] Jungtae Rha, PhD, [3] Adam M. Dubis, [4] Daniela M. O. Bonci, PhD, [4, 5] Alfredo Dubra, PhD,[6] Edwin M. Stone, MD, PhD, [7] Maureen Neitz, PhD, [8] Joseph Carroll, PhD, [3, 4]

Institute affiliations

[1]Department of Ophthalmology and Visual Sciences, University of Illinois at Chicago, Chicago, Illinois, USA.

[2]The Chicago Lighthouse for People Who Are Blind or Visually Impaired, Chicago, Illinois, USA.

[3]Department of Ophthalmology, Medical College of Wisconsin, Milwaukee, Wisconsin, USA.

[4]Department of Cell Biology, Neurobiology & Anatomy, Medical College of Wisconsin, Milwaukee, Wisconsin, USA.

[5]Departamento de Psicologia Experimental, Universidade de Sao Paulo, São Paulo, Brazil.

[6] Flaum Eye Institute, University of Rochester, Rochester, New York, USA.

[7]Department of Ophthalmology and Visual Sciences, Howard Hughes Medical Institute, University of Iowa, Iowa City, Iowa, USA.

[8]Department of Ophthalmology, University of Washington, Seattle, Washington, USA.

Address for correspondence

Gerald A. Fishman, MD

The Chicago Lighthouse for People Who Are Blind or Visually Impaired

1850 West Roosevelt Road

Chicago, IL 60608-1298

Tel: +1-312-997-3666; Fax: +1-312-506-0104; email: gerafish@uic.edu

Acknowledgements

Supported by funds from the Foundation Fighting Blindness, Columbia, Maryland, Grant Healthcare Foundation, Lake Forest, Illinois, unrestricted departmental grants from Research to Prevent Blindness (University of Illinois, University of Washington, and Medical College of Wisconsin), CAPES, NIH grants P30EY001931, P30EY001730, P30EY001792, R01EY017607, & T32EY014537, the Thomas M. Aaberg, Sr., Retina Research Fund, and Hope for Vision. This investigation was conducted in a facility constructed with support from the Research Facilities Improvement Program; grant number C06 RR-RR016511, from the National Center for Research Resources, National Institutes of Health. JC is the recipient of a Career Development Award from Research to Prevent Blindness. Alfredo Dubra holds a career award at the scientific interface from the Burroughs Wellcome Fund.

None of the authors have any proprietary interest in this work.

Total word count for text: 5951 words

Abstract

Purpose. To assess photoreceptor structure and function in patients with congenital achromatopsia.

Methods. Twelve patients were enrolled. All patients underwent a complete ocular examination, spectral-domain OCT (SD-OCT), full-field electroretinographic (ERG), and color vision testing. Macular microperimetry (in 4 patients) and adaptive optics (AO) imaging (in 9 patients) was also performed. Blood was drawn for screening of disease-causing genetic mutations.

Results. Mean (±SD) age was 30.8 (±16.6) years. Mean best-corrected visual acuity was 0.85 (±0.14) log MAR units. Seven patients (58.3%) showed either an absent foveal reflex or non-specific retinal pigment epithelium mottling to mild hypopigmentary changes on fundus examination. Two patients showed an atrophic-appearing macular lesion. On anomaloscopy, only five patients matched over the entire range from 0-73. SD-OCT examination showed a disruption or loss of the macular inner/outer segments (IS/OS) junction of the photoreceptors in 10 patients (83.3%). Seven patients showed an optically empty space at the level of the photoreceptors in the fovea. AO images of the photoreceptor mosaic were highly variable but significantly disrupted from normal. On ERG testing, 10 patients (83.3%) showed evidence of residual cone responses to a single flash stimulus response. The macular microperimetry testing showed that the overall mean retinal sensitivity was significantly lower than normal (12.0 dB vs. 16.9 dB, $p < 0.0001$).

Conclusions. The current approach of using high-resolution techniques to assess photoreceptor structure and function in patients with achromatopsia should be useful in guiding selection of patients for future therapeutic trials as well as monitoring therapeutic response in these trials.

Introduction

Congenital achromatopsia is a genetically heterogeneous, predominately autosomal recessive, retinal disorder with a prevalence of about 1 in 30,000 in the general population.[1] It is characterized by a lack of color discrimination, poor visual acuity, photophobia, pendular nystagmus, and abnormal photopic electroretinographic (ERG) recordings with preservation of the rod-mediated ERG. A prior report by Khan and co-workers showed that the rod ERG function can be modestly subnormal.[2] The disease has been categorized into complete and incomplete achromatopsia subtypes. The incomplete (atypical) form is defined as dyschromatopsia, in which the symptoms are similar to those of the complete achromatopsia (typical) form but with less visual dysfunction.[3] Patients with the complete form have non-detectable cone function on ERG testing, whereas those with the incomplete form retain some residual cone function on ERG, and often more preserved color vision and a higher level of visual acuity (up to 0.20).[3-5] Funduscopy is usually normal in both forms, although not infrequently macular pigmentary mottling and even occasionally atrophic changes have been described.[6]

The known causes of congenital achromatopsia are all due to malfunction of the retinal phototransduction pathway. Specifically, recessive forms of achromatopsia result from the inability of cone photoreceptors to properly respond to a light stimulus by hyperpolarizing. To date, mutations in four genes have been identified to cause achromatopsia in human patients, including the alpha and beta-subunits of the cone cyclic nucleotide-gated ion channels, *CNGA3* (ACHM2, OMIM600053) and *CNGB3* (ACHM3, OMIM605080), which are located in the plasma membrane of the cone outer segments, the alpha-subunit of the cone photoreceptor transducin, *GNAT2* (ACHM4, OMIM139340), and the catalytic alpha-subunit of the cone cyclic

nucleotide phosphodiesterase, *PDE6C* (OMIM600827). The vast majority of human cases of achromatopsia are caused by mutations in either *CNGA3* or *CNGB3*.[7-11] Prior recent reports of animal studies showed that *CNGB3, CNGA3* or *GNAT2* knockout mice and naturally occurring dog models of achromatopsia responded well to adeno-associated virus (AAV) gene therapy. In animal models of human achromatopsia, cone ERG amplitudes recovered to nearly normal levels.[12-14] These results from proof-of-principle experiments in animals with cone-directed gene therapy offer promise for eventual translation to human patients. Identifying and then targeting retinal locations with retained photoreceptors will be a prerequisite for successful gene therapy in achromatopsia patients.

Previous observations regarding photoreceptor structure in achromatopsia have been limited primarily to histological reports. In a previous report by Galezowski,[15] the retinal cones were described as entirely absent. Larsen[16] reported malformed foveal cones with normal cones in the peripheral retina while Harrison et al.[17] found misshaped and reduced numbers of retinal cones. In another report by Falls et al.,[18] normal numbers of odd-shaped foveal cones and isolated numbers of cones in the peripheral retina were described. Glickstein and Heath[19] found no evidence of foveal cones and reduced numbers of peripheral cones. While genetic testing was not available at the time of these studies, they nevertheless highlight the fact that the picture of photoreceptor structure in achromatopsia is likely to be complex. Some clarity on this issue has begun to come from the use of non-invasive imaging techniques to assess photoreceptor structure in patients with achromatopsia. Optical coherence tomography (OCT), which provides excellent axial resolution, has been used to show a highly variable phenotype at the level of the photoreceptor inner segment (IS) and outer segment (OS),[4,6,20,21] though the general interpretation has been that there is an absence or reduction of healthy cone structure. Adaptive

optics (AO) provides high lateral resolution,[22-24] and was used in a single case to examine photoreceptor structure on the single-cell level.[25] The authors visualized a normal rod photoreceptor mosaic, but did not report any evidence of cone structure. These findings only confirm the complexity of the photoreceptor phenotype in achromatopsia, thus warranting further investigation.

Here we used non-invasive high-resolution imaging tools (spectral-domain OCT and AO scanning laser ophthalmoscopy) together with functional measures of vision (ERG, microperimetry, and color vision) to assess photoreceptor structure and function in patients with congenital achromatopsia. We sought to correlate these findings with genetic information from the same subjects. Not only is this approach expected to provide a better understanding of the disease, but also should prove useful in identifying which patients may be most likely to benefit from participating in future gene-targeted treatment trials to rescue or restore cone photoreceptors in this group of patients. Moreover, the structural and functional assays employed here would be useful for evaluating the therapeutic efficacy in patients who in fact go on to receive intervention.

Methods and Materials

Participants

Twelve patients (24 eyes) with congenital achromatopsia were included in the study, 7 were males (58.3%) and 5 were females (41.7%). The mean (± SD) age of the patients was 30.8 (±16.6) years with a range from 13 to 55 years. There were 6 Caucasian (50.0%), 2 Hispanic (16.7%), 3 of Middle Eastern ancestry (25.0%) (2 Jordanian, 1 Lebanese) and 1 African

American (8.3 %) enrolled in the study. Informed consent was obtained from all participants. All study patients underwent a complete ocular examination, spectral-domain OCT (SD-OCT), full-field ERG, color vision testing, macular microperimetry (in 4 patients), and AO imaging (in 9 patients). Blood was drawn for screening of disease-causing genetic mutations.

The clinical testing portion of the study was conducted in the Department of Ophthalmology at the University of Illinois at Chicago and the Chicago Lighthouse for People Who Are Blind or Visually Impaired, while the AO imaging and additional OCT measurements were performed in the Department of Ophthalmology at the Medical College of Wisconsin. The screening for genetic mutations was performed by the Carver Nonprofit Genetic testing Laboratory at the University of Iowa and additionally at both the Medical College of Wisconsin and the University of Washington. The current study followed the tenets of the Declaration of Helsinki and it was approved by institutional review boards at the University of Illinois, the Medical College of Wisconsin, the University of Rochester, and the University of Washington.

The diagnosis of achromatopsia was based on the history of a decrease in central vision, photophobia, markedly impaired color vision, nystagmus within the first decade of life, and abnormal cone responses on ERG recordings with most often normal, but occasionally subnormal, rod responses. Patients with a diagnosis of achromatopsia who were seen, from August, 2008, through February, 2011, by two of the authors (M.A.G. and G.A.F.) during their routine clinical follow-up examinations were included in the current prospective study if they were willing to undergo the study protocol testing. Additional patients previously seen by one of the authors (G.A.F.) were contacted by telephone and asked to participate in the study based on their prior diagnosis of achromatopsia.

Exclusion criteria included an inability to maintain moderately steady fixation, posterior uveitis, diabetic retinopathy, optic neuropathies, spherical refraction of more than ± 6 diopter (D) or cylinder refraction of ± 2 D, or any central media opacity sufficient to hinder OCT and/or AO examinations. No patients with a history of any systemic diseases such as hypertension or diabetes mellitus were included. A summary of tests performed on each subject is given in **Table 1**.

Ocular Examination

Complete eye examination, included best-corrected visual acuity (BCVA) using an Early Treatment Diabetic Retinopathy Study (ETDRS) chart (The Lighthouse, Long Island City, New York, USA), slit-lamp biomicroscopic examination of the anterior segment, and intraocular pressure (IOP) measurement with Goldmann applanation tonometry. Both eyes were dilated with phenylephrine 2.5% and tropicamide 1%. Fundus examination was performed using both direct and indirect ophthalmoscopy as well as biomicroscopy with a noncontact 78 diopter lens.

Electroretinogram Examination

A full-field electroretinogram (ERG) was obtained monocularly with the use of a unipolar Burian-Allen contact lens electrode. One eye was tested after pupil dilation. The ERG responses were obtained according to the International Society for Clinical Electrophysiology of Vision (ISCEV) guidelines[26] that included a dark-adapted rod-isolated response, a dark-adapted rod-dominant response, 32-Hz flicker response, and a light-adapted single flash response. Parameters included amplitudes and implicit times for each of the major waveform components. All results

were compared with 90% tolerance limits or an appropriate range for a visually normal population.

Color Vision Testing

All study patients underwent testing by using Ishihara pseudoisochromatic plates and Rayleigh match (HMC OCULUS anomaloscope, OCULUS Optikgeräte GmbH, Wetzlar, Germany), in which patients were asked to match a yellow monochromatic light in one test field of a bipartite stimulus with a mixture of various proportions of green and red lights in another portion of the bipartite field, by varying the proportion in the color mix. The average normal width of the Rayleigh match was about two units with a range of five units; therefore, an equation width greater than five units was considered to be abnormal.[27] The most frequent average midpoint, as provided by the manufacturer, is a red-green ratio setting of 40 with a range of 34-46.

Optical Coherence Tomography (OCT) Examination Protocols

All subjects included in the study underwent OCT examinations by using either a Fourier-domain (FD-OCT) system (The Optovue technology, RTvue, version 3.5; Optovue Inc, Fremont, California, USA) or a SD-OCT/SLO system (OPKO instrumentations, Miami, Florida, USA).

The examination protocols used for scanning the macula were as follows; in the Optovue system, the MM5 and Radial Lines protocols were used for image acquisition, where the radial scan consisted of twelve 6-mm radial scans at 15° polar intervals passing through the center of the fovea. All 12 scans were acquired simultaneously, and the total time taken for their acquisition was 0.27 seconds. Each radial line consisted of 1024 A-scans. The MM5 scan protocol consisted of a raster protocol of 5 x 5 mm centered at the fovea, with a total acquisition

time of 0.78 seconds. Scans were accepted only if they had a signal strength index greater than 35 and were free of artifacts.

For the OPKO system, both the Line scan (B-scan) and the 3D Retinal Topography scan protocols were used for image acquisition. The Line scan mode allows the capture of high-resolution cross-sectional B-scan OCT images of the vitreoretinal, retinal, and chorioretinal structures. The 3D Retinal Topography mode covers an area of 9.0 x 9.0 mm with a 2.0 mm depth.

The retinal thickness map is displayed as nine ETDRS-like subfields including central, parafoveal and perifoveal superior, temporal, inferior, and nasal subfields. The central subfield included the circle centered on the fovea with a radius of 0.5 mm. The parafoveal subfields included the concentric ring of retina around the central subfield with an inner radius of 0.5 mm and an outer radius of 1.5mm from the fovea. The perifoveal subfields included the outer ring of retina beyond the parafoveal subfields concentric with the fovea and with an inner radius of 1.5 mm and an outer radius of 3 mm. The macular thickness data were compared with normative data provided by the manufacturers, comprised of 225 eyes of 119 normative control subjects (mean age of 47.8±16.3 years) for OPKO system and 268 eyes of 134 normative control subjects (mean age of 44.1±15.5 years) for the Optovue system. The data acquired by both the Optovue and OPKO OCTs are used for analysis in the present manuscript. All patients were able to perform the examination without any difficulty either due to a nystagmus that was mild in most of the patients or photoaversion problems.

For nine subjects, during AO imaging at the Medical College of Wisconsin, additional images of the macula were obtained using a high-resolution SD-OCT (Bioptigen, Inc., Durham, North Carolina, USA). Line scan sets were acquired (1000 A-scans / B-scan; 100 repeated B-scans) through the foveal center, and this location was confirmed based on inspection of the accompanying high-density volume scan. Scans were registered and averaged as previously described to reduce speckle noise in the image.[28]

Adaptive Optics Imaging

Each subjects' eye was dilated and accommodation suspended using one drop each of phenylephrine 2.5% and tropicamide 1 %. Images of the central retina were obtained using one of two imaging systems housed at the Medical College of Wisconsin, either an AO flood-illuminated camera or an AO scanning laser ophthalmoscope (AOSLO). Subject 5 underwent imaging on both devices. System details for the AO camera[29] and AOSLO[30] have been previously published. The AO flood-illuminated camera operates at 167 frames per second and utilizes a 52-channel deformable mirror (Imagine Eyes, Orsay, France), while the AOSLO operates at 14 frames per second and utilizes a 97-channel deformable mirror (ALPAO, Biviers, France). Flood-illuminated AO images were processed according to previously published methods, with multiple images being registered and averaged in order to improve the image contrast.[29] For the AOSLO, a desinusoiding algorithm was applied to each video sequence and individual frames were then selected for analysis. No filtering of any kind was applied to these images. From these processed images, rod and cone density was estimated using a direct counting procedure.[31,32] In all cases, the approximate retinal location of the photoreceptor images relative to the foveal center was determined based on the fundus images using common blood

vessel patterns and the subjects' suspected locus of fixation (derived from the volumetric OCT images).

Macular Sensitivity Testing by Microperimetry (MP)

MP was performed on four achromatopsia patients using the Spectral OCT/SLO microperimetry system (OPKO Instrumentations, Miami, Florida, USA). This instrument allows the examiner to view the fundus on a computer monitor while it is imaged in real time by an SLO fundus camera. Background luminance was set at 10 cd/m^2. Stimulus intensity can be varied in 1dB (0.1 log) steps from 0 to 20, where 0 dB represents the brightest luminance of 125 cd/m^2. The system also incorporates an automated tracking system to compensate for eye movement during examination.

The testing was conducted in a darkened room that minimized the photoaversion commonly experienced by achromatopsia patients. All patients underwent brief training at the beginning of MP testing allowing familiarization and practice with correct operation of the response trigger and the stimulus target. This was followed immediately by the actual test. All tests were performed after pupil dilatation. Patching of the non-tested eye was performed. The patients were instructed to fixate on a red square as a fixation target and press a button once they saw the stimulus target. A standard grid pattern (Polar 3) composed of 28 points arranged in three concentric circles (2.3°, 6.6°, and 11° in diameter) within the central macula was used. The inner circle is composed of four points, whereas the middle and outer circles are each composed of 12 points. Parameters included a Goldmann III size stimulus, 200ms stimulus duration, and test strategy 4-2. The individual sensitivity values at 28 different loci within the central 12 degrees were compared to normative data, which was retrieved from 32 visually normal subjects.[33]

Molecular Analysis

For subjects 1-5, and 7-9 **(Table 2)**, DNA was isolated from whole blood and used in the polymerase chain reaction (PCR) in the Neitz Lab at the Medical College of Wisconsin, or at the University of Washington. Mutation screening was performed on exons and intron/exon junctions of the genes encoding the alpha-subunit of cone transducin (*GNAT2*), and the genes encoding the alpha-subunit (*CNGA3*) and beta-subunit (*CNGB3*) of the cone cyclic nucleotide gated ion channel. Exon 18 of the *CNGB3* was not analyzed. Individual exons or pairs of adjacent exons and the intron/exon junctions for each gene were amplified, and both strands of the resulting PCR products were directly sequenced. Sequencing was performed using the AmpliTaq FS kit and reactions were analyzed on the ABI 3130xls genetic analyzer.

For subjects 1-5, and 7-9, independent genetic analysis was conducted by the Carver Laboratory at the University of Iowa on the exons for the *CNGA3* and *CNGB3* genes. Additionally, DNA from blood samples were obtained from subjects 6, 10-12 and analyzed in the Carver Lab, DNA was extracted by following the manufacturer's specifications for whole blood DNA extraction using Gentra Systems' Autopure LS instrument. Automated bi-directional DNA sequencing of the coding sequences of *CNGA3* and *CNGB3* was performed using an ABI 3730 sequencer. Exon 18 of the *CNGB3* gene was sequenced for all subjects in the Carver Lab.

Results

Clinical Examination

The average best-corrected visual acuity was 0.88 log MAR units with a SD of 0.14 (range, 0.44-0.96), equivalent to 20/55-20/186 on a Snellen acuity chart. Subjectively, all patients had a past history of pendular nystagmus dated since birth that improved over time. The degree of photoaversion was mild in 2 patients and moderate to severe in 10 patients.

Fundus examination in our study cohort showed 3 patients (25.0%) with a normal macular morphology and normal-appearing foveal reflex (mean age of 14.7 years, range from 13 to 17 years), 5 patients (41.7%) showed a blunted (absent) foveal reflex (mean age of 28.6 years, range from 15 to 50 years), and 2 patients (16.7%) showed evidence of macular lesions in the form of retinal pigment epithelium (RPE) mottling, mild hypopigmentary changes in the fovea/parafoveal regions, or a few, punctate, hard drusen in each eye (ages 27 and 55 years). In addition, 2 patients (16.7%) showed a well-circumscribed atrophic-appearing macular lesion in each eye (ages 49 and 52 years) (**Table 1**).

Genetic Analysis

Our genetic testing results showed that 11 out of 12 patients had a positive genetic mutation in either the *CNGB3* or *CNGA3* gene, which was similar to previous reports.[8,37,40] Mutations were independently confirmed in the Carver Lab and Neitz Lab for subjects 1-5, and 7-9. The other subjects were sequenced only in the Carver Lab. The genetic results are summarized in **Table 2**.

The achromatopsia phenotype for subjects 5, 7, and 8 can be attributed to each of these subjects being homozygous for a frame shift mutation in exon 10 of the *CNGB3* gene in which

residue C 1148 in codon 383 is deleted.[4,8] Subject 4 is homozygous for a missense mutation in the *CNGA3* gene at codon 570 (Ser570Ile). Subjects 2, 6, 9, 11, and 12 are each compound heterozygotes for two different mutations within the *CNGA3* gene. For subject 2, one mutation changes codon 221 from arginine to a premature translational termination codon, the second mutation is a previously identified pathogenic missense mutation (Arg277His).[7] Subjects 6 and 12 were found to have a new mutation (Gly329Cys) and a previously identified mutation (Arg436Trp).[4,34,35] Subject 9 has two different missense mutations in the cGMP binding domain of *CNGA3*. These include a new mutation (Asp514Val) and a previously identified mutation, (Arg410Trp).[4,34,35] Subject 11 has two previously described mutations, Arg283Gln and Arg436Trp.[4,34,35] Subjects 3 and 10 are both heterozygous for the one base deletion at position 1148 of the *CNGB3* gene, however a second mutation was not found in *CNGB3* or *CNGA3* for either subject or in the *GNAT2* gene for subject 3. The *GNAT2* gene was not evaluated for subject 11. For subject 1, clearly pathogenic mutation(s) in *CNGA3*, *CNGB3*, or *GNAT2* were not found.

Color Vision Results

Color vision screening with Ishihara color plates showed the ability to identify only the test plate in 6 patients (50.0%) while 6 patients (50.0%) could identify plates from 1-5. Anomaloscopic examination showed an abnormality consisting most commonly of a shift of the Rayleigh match mid-point towards the red end of the color spectrum with an average midpoint of 54 and an abnormal equation width in 7 patients (58.3%) while 5 patients (41.7%) matched at the entire range of the anomaloscope from 0-73. The red-green half of the anomaloscopic field appeared

dim at longer wavelengths and substantially brighter at shorter wavelengths in most of the study patients (n=9).

Assessing Photoreceptor Function: Electroretinogram Findings

Full-field electroretinogram (ERG) recordings were obtained on all of the study patients. The isolated rod response was normal in 9 patients (75.0 %) with an average amplitude of 387.7 μV (lower limit of normal is 273 μV) while 3 patients (25.0%) showed an average reduction of 31% below the lower limit of normal with an average amplitude of 187.3 μV. The maximum dark-adapted response after 30 minutes was normal in 6 patients (50.0%) with an average amplitude of 559.8 μV (lower limit of normal is 460.9 μV) while 6 patients (50.0%) showed an average reduction of 24% below the lower limit of normal with an average amplitude of 351.4 μV. The single flash light-adapted response was non-detectable in 2 patients (16.7 %) while 10 patients (83.3%) showed a markedly reduced b-wave response with average amplitude of 34.9 μV (lower limit of normal is 132.8 μV). All patients showed non-detectable responses to a 32-Hz flicker stimulus.

Microperimetry Results

Macular microperimetry testing was performed on 8 eyes of 4 patients (mean age of 19.0 years, range 14-30 years), and the results were compared to 32 visually normal subjects (mean age 41.6 years, range 28-66 years) on the same SD-OCT/SLO system used in this study.[33]

The MP testing showed that the overall mean retinal sensitivity in our currently studied patients was significantly less than that of controls (12.0 dB vs. 16.9 dB, $p < 0.0001$, Student's t-test was used for statistical analysis). Microperimetry testing of 28 individual points within a 6

degree radius from the center of the foveola (12 degree circle, Polar 3 pattern) showed areas of subnormal individual point sensitivities that were below the 95 and 99% confidence limits of normal sensitivity. In addition, the 4 patients studied showed relatively stable central fixation in each eye (81% of eye movements were within 2 degrees around the projected fixation target while 92 % were within 4 degrees) **(Figure 1)**. The structural and functional characteristics of these 4 patients are shown in **Table 1**.

Retinal Morphology in Achromatopsia: SD-OCT Results

Regarding the SD-OCT examination, 2 patients (16.7%) (ages 13 and 17 years) showed normal macular structures with an intact IS/OS junction of the photoreceptors and grossly normal-appearing outer nuclear layer (ONL) thickness. Six patients (50.0%) showed a shallow and broad foveal depression (possibly reflecting a degree of foveal hypoplasia or mal-development) [32] with continuation of the inner plexiform layer (IPL) and outer plexiform layer (OPL) to within the foveolar region **(Figure 2)**. Ten patients (83.3 %) showed focal disruption and/or loss of the IS/OS junction of the photoreceptors and RPE layer attenuation within the macular region (mean age 34.0 years, range from 14 to 55 years). Seven out of those 10 patients showed the presence of an optically empty space (punched-out hyporeflective space) at the level of IS/OS junction of the photoreceptors that corresponded to disruption and/or loss of the photoreceptor layer **(Figure 2)**.

By a quantitative method of analysis, on OCT examination, 11 eyes (45.8%) of 6 patients showed a normal central foveal subfield thickness with an average thickness of 259.0±11.7 μm (mean age of 22.7 years, range from 13 to 50 years). Thirteen eyes (54.2%) of 7 patients showed thinning in the central foveal subfield with an average thickness of 193.8±25.7 μm (mean age of

32.8 years, range from 14 to 55 years), which was significantly thinner statistically than normal ($p< 0.0001$, Student's t-test was used for statistical analysis). The data used for measurement of the macular thickness were obtained from both Optovue and OPKO systems.

Photoreceptor Structure Assessed with Adaptive Optics Imaging

The AO images of the photoreceptor mosaic were highly variable, both in image quality and in the appearance of the mosaic itself. In all cases, the mosaic was significantly disrupted from normal **(Figure 3)**. In the normal retina, peripheral cones appear as bright spots with a dark ring, and in some cases this central bright spot is missing (arrows, panel b). We posit that the dark ring is the inner segment of the cone, while the central reflection is derived from the outer segment or IS/OS junction. These images are critical to interpreting the findings in patients with achromatopsia, as we observed residual cone inner segment structure in all but one of the subjects imaged. In fact, in three individuals (subjects 5, 10, 12 in **Table 2**) we found cones that had a subtle central reflective structure within the inner segment, suggesting improved structural integrity of the outer segment relative to the other patients. It may be that the presence/absence of this structure, or its intensity, could be an indicator of relative cone structural health.

We were able to acquire images at about 10 degrees from the fovea in 2 subjects **(Figure 3D and 3E)**, and found quite different degrees of residual cone structure, though both appeared reduced compared to the normal image at 10 degrees from the fovea **(Figure 3B)**. In all images, the cross sectional profiles of individual rods and cones appeared consistent with that previously reported.[25] In one subject (subject 5 in **Table 2**) we were able to map the border of his central IS/OS disruption **(see Figure 4)**. Given the size of the disruption (201 μm), we believe that this

represents the rod-free zone in this individual, as it is consistent with previous estimates of this structure.[36]

In another subject (subject 12 in **Table 2**) we were able to examine multiple locations of known distance from the fovea. While no obvious cone structure could be seen in the central fovea, cone inner segments were present at 2, 4, and 16 degrees eccentricity; though they were least numerous at 16 degrees **(Figure 5)**.

Discussion

Macular Structure in Achromatopsia

We used a variety of techniques to assess macular structure in patients with achromatopsia. The value of fundus imaging techniques in assessing achromatopsia patients has been described in previous studies.[6,20,21,25] In our study cohort of 12 patients afflicted with achromatopsia, 7 patients (58.3%) showed evidence of minor macular changes on fundus examination that varied from either an absent foveal reflex or non-specific RPE mottling to mild hypopigmentary changes. Two patients showed a well-circumscribed atrophic-appearing macular lesion while three patients did not show any clinically apparent macular changes. These findings were similar to two recent reports[4,37] that showed macular changes in achromatopsia patients.

Three anatomical features of the macula can be examined using SD-OCT imaging –the appearance of the photoreceptor layer (external limiting membrane (ELM) and IS/OS), macular thickness, and foveal morphology. Our findings were generally consistent with previous reports, adding to the current picture of significant structural variability in achromatopsia patients. Ten patients in our cohort showed a disruption or loss of the IS/OS junction of the photoreceptors in

the macula. The presence of an optically empty space (punched-out hyporeflective space) at the level of the photoreceptors in the fovea was observed in seven patients (mean age of 32.1 years). This has been observed previously by others in patients where no genetic subtype was identified.[6,38,39] The exact mechanism for the foveal optically empty space and disrupted IS/OS junction of the photoreceptor layer is not currently known. One hypothesis is that it might be due to autolysis of cone photoreceptor outer segments or ineffective phagocytosis of degenerative photoreceptor cell debris.

In contrast, two of the younger patients (ages 13 and 17 years) showed a normal macular structure with a generally intact IS/OS junction of the photoreceptors and normal-appearing ONL thickness. This general difference in IS/OS structure is consistent with the findings presented by Thiadens et al.,[6] who reported loss of the IS/OS junction with a disruption of the ciliary layer (the connecting cilium of the photoreceptors) on OCT initially, followed by the appearance of an evolving bubble in the photoreceptor layer and thinning or atrophic-appearing changes of the RPE in older patients with achromatopsia. Eleven eyes (45.8%) of 6 patients showed a normal foveal subfield thickness while 13 eyes (54.2%) of 7 patients showed a thinning of the foveal subfield thickness on OCT examination. This variability is consistent with findings reported previously[6,20,21] and may be due to differences in age and/or genotype. Six of our patients had a broad and shallow foveal depression with preservation of inner retinal layers through the foveal center, similar to that seen in some individuals with albinism.[32] Foveal hypoplasia is recognized as a relatively common feature of achromatopsia,[4,6,40] though the significance of this finding as it pertains to the etiology of achromatopsia remains to be defined.

Adaptive optics (AO) permits direct visualization of individual rod and cone photoreceptors.[41,42] It is becoming appreciated that in a variety of diseases, AO can reveal cellular disruption in areas that appear normal with conventional imaging tools (including SD-OCT).[43-45] We directly examined photoreceptor structure in nine subjects using AO, and observed residual cone inner segment structure in all but one of the subjects imaged. In three individuals (subjects 5, 10, 12) we even observed cones that had a subtle central reflective structure within the inner segment, suggesting improved structural integrity of the outer segment relative to the other patients. The variable appearance of the residual cones may be an indicator of relative cone structural health, though this requires further investigation. That we see cone structure even in the oldest patient (55 years old) suggests that while there may be general advancement of the disease with age, there is not complete loss of cone structure. Thus the therapeutic window may be larger than that inferred from recent SD-OCT studies.[6] Interestingly, there was nothing unique about these three subjects' SD-OCT images, highlighting that it may not be possible to directly infer the degree of cone structure from SD-OCT imaging alone. This was perhaps most notable in subject 12, where in areas that lacked a robust IS/OS layer, we still observed numerous cone IS structures. It would be of interest to image with AO individuals receiving gene therapy intervention, as AO imaging (specifically the appearance of the cone reflection profile) may provide the most sensitive biomarker for assessing a treatment response in patients receiving therapeutic intervention for achromatopsia. In addition, in future longitudinal studies, it would be useful to assess how cone structure changes over time with AO and SD-OCT.

Residual Cone Function in Achromatopsia

We observed significant residual cone function in our patients-albeit to a variable degree. Regarding color vision (a cone-mediated process), only 5 of the 12 patients matched the entire range of red/green mixtures on the anomaloscope, while 7 patients showed a midpoint shifted towards the red end of the Rayleigh match, which has been reported previously in incomplete achromatopsia.[46] Out of those 5 patients who matched over the entire range of anomaloscope, all patients showed a non-detectable (ND) light-adapted flicker response, 2 of the 5 patients showed a non-detectable single flash light-adapted response, while 3 patients showed an average b-wave amplitude of 35.9 μV to a single flash light-adapted response with a lower limit of normal of 132.8 μV. Out of those patients who showed a shift in their match point into the red portion of the color spectrum (n=7), all showed ND responses to the flicker stimulus, while all patients showed residual cone function to the single flash light-adapted stimulus with an average of 32.9 μV and a range of 26.0 to 43.0 μV (lower limit of normal is 132.8 μV). Regarding the photopic ERG in our entire study cohort, 10 patients (83.3%) showed evidence of residual cone responses to a single flash stimulus response while all patients showed non-detectable responses to a flicker stimulus. In addition, the rod responses were normal in 9 patients, while 3 patients showed almost an average of a 31% reduction below the lower limit of normal, which was similar to a previous report by Khan et al.[2] who showed an abnormality of scotopic ERG responses in achromatopsia patients. Finally, the mean sensitivity on macular microperimetry of 12.0 dB is consistent with the presence of residual cone function. Taken together, these functional findings further support the notion that achromatopsia patients can have substantial residual cone function, which is in accordance with prior reports.[4,5]

Genotype-Phenotype Correlations in Achromatopsia

Prior reports showed that mutations in the *CNGA3* and *CNGB3* genes are the most frequent mutations encountered in patients with achromatopsia.[8,38,47] Consistent with this, disease-causing mutations in *CNGA3* and *CNGB3* genes were observed in 11 out of 12 of our patients. A limitation of the current study is the relatively small number of subjects and the diverse genotypes (including an absence of disease-causing mutations in one patient), making it impossible to draw firm conclusions about genotype-phenotype relationships. That said, we did not observe any distinguishing clinical, psychophysical, electrophysiological, or structural (SD-OCT / AO) features in patients with *CNGB3* versus *CNGA3* mutations. None of our patients were found to have a mutation(s) in the *GNAT2* gene, so it remains unclear whether such patients might show any systematic differences in cone structure and function. The unifying finding is that there is substantial variation in phenotype, *even within individuals with the same genotype*. Three unrelated patients in our study (subjects 5, 7, 8 in **Table 1 and 2;** ages 15, 27, and 49 years, respectively) showed the same homozygous mutation in the *CNGB3* gene, however their phenotypic findings differed. The 15-year-old patient showed a normal-appearing fundus examination and non-detectable cone responses to both single-flash light-adapted and 32-Hz flicker stimuli with normal rod response on ERG testing. The 27-year-old patient showed a foveal hypopigmented lesion and non-detectable (to 32-Hz flicker) and markedly reduced (to single flash light-adapted) cone responses with normal rod responses on ERG testing, while the 49-year-old patient showed an atrophic-appearing macular lesion on fundus examination and non-detectable (to 32-Hz flicker) and markedly reduced (to single flash light-adapted) cone responses with normal rod responses on ERG testing. Two of our study patients are siblings

(subjects 6, 12 in **Table 1 and 2**, ages 17, 14 years, respectively) and carry the same heterozygous mutations in the *CNGA3* gene without any differences in their phenotype, both clinically and electrophysiologically. However, subject 12 showed more loss of foveal IS/OS junction of the photoreceptors than his older sister (subject 6) on OCT testing **(Figure 1)**. Since our study was not intended to identify longitudinal changes in either retinal structure or function in our patients, we cannot meaningfully address whether any of our differences between individuals with the same genotype support or refute the proposed progressive degeneration reported by Thiadens et al.[6] or whether they represent the effect of an unidentified modifying factor. The issue of progressive loss of cones in achromatopsia remains an important unresolved issue, and will only be settled with additional longitudinal imaging studies on patients of known genotype and/or much larger cross-sectional studies.

Our findings are generally consistent with Nishiguchi et al.,[4] who reported residual cone structure in all of achromatopsia patients they examined, but found no obvious correlation between the specific genotype and the severity of cone dysfunction. In addition, subjects 5 (*CNGB3*) and 12 (*CNGA3*) had more substantial cone structure in their AO images with many cones containing a reflective core (presumed OS in origin). This demonstrates that significant cone structure can remain in the two main genotypes, though further work is needed to determine whether there is any significant difference between individuals harboring different mutations within each genotype. Taken together, these findings indicate that genetic analysis alone may not be sufficient to identify the best candidates for a given gene therapy intervention.

Implications for Improving the Success of Gene Therapy in Humans

In studies of animal models of human achromatopsia, AAV-mediated gene therapy was shown to recover cone ERG-amplitudes to near normal levels.[12-14] There is justified enthusiasm surrounding the prospect of translating these proof-of-principle experiments in animals to the treatment of human patients. We feel that the combined assessment of photoreceptor structure and function outlined here will be important to ultimately improving the success of such intervention and help to identify the best candidates for a specific therapy. For example, in a group of patients with retinitis pigmentosa, Talcott et al.[48] recently demonstrated that imaging of the cone mosaic with AOSLO showed improvements in cone structure in response to ciliary neurotrophic factor (CNTF) treatment that were not visible using conventional assays. We anticipate that application of similar high-resolution imaging techniques and sensitive measures of retinal function will provide a more sensitive evaluation of therapeutic efficacy in clinical trials for patients with achromatopsia.

References

1. Sharpe LT, Stockman A, Jagle H et al. Opsin genes, cone photopigments and colour blindness. In: Gegenfurtner K, Sharpe LT, eds. Color vision: from genes to perception. Cambridge: Cambridge University Press. 1999: 3-52.
2. Khan NW, Wissinger B, Kohl S, Sieving PA. *CNGB3* achromatopsia with progressive loss of residual cone function and impaired rod-mediated function. Invest Ophthalmol Vis Sci. 2007; 48(8): 3864-3871.
3. Pokorny J, Smith VC, Pinckers AJ, Cozijnsen M. Classification of complete and incomplete autosomal recessive achromatopsia. Graefes Arch Clin Exp Ophthalmol. 1982; 219(3):121-130.
4. Nishiguchi KM, Sandberg MA, Gorji N, et al. Cone cGMPgated channel mutations and clinical findings in patients with achromatopsia, macular degeneration, and other hereditary cone diseases. Hum Mutat. 2005; 25(3):248-258.
5. Michaelides M, Hardcastle AJ, Hunt DM, Moore AT. Progressive cone and cone-rod dystrophies: phenotypes and underlying molecular genetic basis. Surv Ophthalmol. 2006; 51(3):232-258.
6. Thiadens AA, Somervuo V, van den Born LI, et al. Progressive loss of cones in achromatopsia: an imaging study using spectral-domain optical coherence tomography. Invest Ophthalmol Vis Sci. 2010; 51(11):5952-5957.
7. Wissinger B, Gamer D, Jägle H, et al. CNGA3 mutations in hereditary cone photoreceptor disorders. Am J Hum Genet. 2001; 69(4):722-737.
8. Kohl S, Baumann B, Broghammer M, et al. Mutations in the CNGB3 gene encoding the beta-subunit of the cone photoreceptor cGMP-gated channel are responsible for

achromatopsia (ACHM3) linked to chromosome 8q21. Hum Mol Genet. 2000; 9(14):2107-2116.

9. Chang B, Dacey MS, Hawes NL, et al. Cone photoreceptor function loss-3, a novel mouse model of achromatopsia due to a mutation in Gnat2. Invest Ophthalmol Vis Sci. 2006; 47(11):5017-5021.
10. Rosenberg T, Baumann B, Kohl S, Zrenner E, Jorgensen AL, Wissinger B. Variant phenotypes of incomplete achromatopsia in two cousins with GNAT2 gene mutations. Invest Ophthalmol Vis Sci. 2004; 45(12):4256-4262.
11. Thiadens AAHJ, den Hollander AI, Roosing S, et al. Homozygosity mapping reveals PDE6C mutations in patients with early-onset cone photoreceptor disorders. Am J Hum Genet. 2009; 85(2):240-247.
12. Komáromy AM, Alexander JJ, Rowlan JS, et al. Gene therapy rescues cone function in congenital achromatopsia. Hum Mol Genet. 2010; 19(13):2581-2593.
13. Alexander JJ, Umino Y, Everhart D, et al. Restoration of cone vision in a mouse model of achromatopsia. Nat Med. 2007; 13(6):685-687.
14. Pang JJ, Alexander JJ, Lei B, et al. Achromatopsia as a potential candidate for gene therapy. Adv Exp Med Biol. 2010; 664:639-646.
15. Galezowski X. Du diagnostic des Maladies des Yeux par la Chromatoscopie rétinienne: Précéde d'une Etude sur les Lois physiques et physiologiques des Couleurs, J.B. Baillière et Fils, Paris 1868.
16. Larsen H. Demonstration mikroskopischer Präparate von einem monochromatischen Auge. Klinische monatsblätter für augenheilkunde 1921; 67:301-302.

17. Harrison R, Hoefnagel D, Hayward JN. Congenital total color blindness, a clinicopathological report. Arch Ophthalmol. 1960; 64: 685-692.
18. Falls HF, Wolter R, Alpern M. Typical total monochromasy-A histological and psychophysical study. Arch Ophthalmol. 1965; 74(5): 610-616.
19. Glickstein M, Heath GG. Receptors in the monochromat eye. Vision Res. 1975; 15(6):633-636.
20. Barthelmes D, Sutter FK, Kurz-Levin MM, et al. Quantitative analysis of OCT characteristics in patients with achromatopsia and blue-cone monochromatism. Invest Ophthalmol Vis Sci. 2006; 47(3):1161-1166.
21. Varsányi B, Somfai GM, Lesch B, Vámos R, Farkas A. Optical coherence tomography of the macula in congenital achromatopsia. Invest Ophthalmol Vis Sci. 2007; 48(5):2249-2253.
22. Liang JZ, Williams DR, Miller DT. Supernormal vision and high-resolution retinal imaging through adaptive optics. J. Opt. Soc. Am. A. 1997; 14(11):2884-2892.
23. Roorda A. Applications of adaptive optics scanning laser ophthalmoscopy. Optom Vis Sci. 2010; 87(4):260-268.
24. Godara P, Dubis AM, Roorda A, Duncan JL, Carroll J. Adaptive optics retinal imaging: emerging clinical applications. Optom Vis Sci. 2010; 87(12):930-941.
25. Carroll J, Choi SS, Williams DR. In vivo imaging of the photoreceptor mosaic of a rod monochromat. Vision Res. 2008; 48(26):2564-2568.
26. Marmor MF, Holder GE, Seeliger NW, Yamamoto S. Standard for clinical electroretinography (2003 update). Doc Ophthalmol. 2004; 108:107-114.

27. Krill AE, Fishman GA. Acquired color vision defects. Trans Am Acad Ophthalmol Otolaryngol. 1971; 75(5):1095-1111.
28. Tanna H, Dubis AM, Ayub N, et al. Retinal imaging using commercial broadband optical coherence tomography. Br J Ophthalmol. 2010; 94(3):372-376.
29. Rha J, Schroeder B, Godara P, Carroll J. Variable optical activation of human cone photoreceptors visualized using a short coherence light source. Opt Lett. 2009; 34(24):3782-3784.
30. Dubra A, Sulai Y. Reflective afocal broadband adaptive optics scanning ophthalmoscope. Biomed Opt Express. 2011; 2(6):1757-1768.
31. Li KY, Roorda A. Automated identification of cone photoreceptors in adaptive optics retinal images. J Opt Soc Am A Opt Image Sci Vis. 2007; 24(5):1358-1363.
32. McAllister JT, Dubis AM, Tait DM, et al. Arrested development: high-resolution imaging of foveal morphology in albinism. Vision Res. 2010; 50(8):810-817.
33. Anastasakis A, McAnany JJ, Fishman GA, Seiple WH. Clinical value, normative retinal sensitivity values, and intrasession repeatability using a spectral-domain OCT/SLO microperimeter. Eye (Lond). 2011; 25(2):245-251.
34. Kohl S, Marx T, Giddings I, et al. Total colour blindness is caused by mutations in the gene encoding the alpha-subunit of the cone photoreceptor cGMP-gated cation channel. Nat Genet. 1998; 19(3):257-259.
35. Wissinger B, Gamer D, Jägle H, et al. CNGA3 mutations in hereditary cone photoreceptor disorders. Am J Hum Genet. 2001; 69(4):722-737.
36. Curcio CA, Sloan KR, Kalina RE, Hendrickson AE. Human photoreceptor topography. J Comp Neurol. 1990; 292(4):497-523.

37. Thiadens AA, Slingerland NW, Roosing S, et al. Genetic etiology and clinical consequences of complete and incomplete achromatopsia. Ophthalmology 2009; 116(10):1984-1989.

38. Grau T, Artemyev NO, Rosenberg T, et al. Decreased catalytic activity and altered activation properties of PDE6C mutants associated with autosomal recessive achromatopsia. Hum Mol Genet. 2011; 20(4):719-730.

39. Thiadens AA, den Hollander AI, Roosing S, et al. Homozygosity mapping reveals PDE6C mutations in patients with early-onset cone photoreceptor disorders. Am J Hum Genet. 2009; 85(2):240-247.

40. Thomas MG, Kumar A, Kohl S, Proudlock FA, Gottlob I. High-resolution in vivo imaging in achromatopsia. Ophthalmology. 2011; 118(5):882-888.

41. Rossi EA, Chung M, Dubra A, Hunter JJ, Merigan WH, Williams DR. Imaging retinal mosaics in the living eye. Eye (Lond). 2011; 25(3):301-308.

42. Dubra A, Sulai Y, Norris JL, et al. Noninvasive imaging of the human rod photoreceptor mosaic using a confocal adaptive optics scanning ophthalmoscope. Biomed Opt Express. 2011; 2(7):1864-1876.

43. Rha J, Dubis AM, Wagner-Schuman M, et al. Spectral domain optical coherence tomography and adaptive optics: imaging photoreceptor layer morphology to interpret preclinical phenotypes. Adv Exp Med Biol. 2010; 664:309-316.

44. Stepien KE, Han DP, Schell J, Godara P, Rha J, Carroll J. Spectral-domain optical coherence tomography and adaptive optics may detect hydroxychloroquine retinal toxicity before symptomatic vision loss. Trans Am Ophthalmol Soc. 2009; 107:28-33.

45. Stepien KE, Martinez WM, Dubis AM, Cooper RF, Dubra A, Carroll J. Detection of photoreceptor disruption after commotio retinae using adaptive optics scanning laser ophthalmoscopy. Invest. Ophthalmol. Vis. Sci. 2011; Suppl. 52: E-Abstract 6657.
46. Smith VC, Pokorny J, Newell FW. Autosomal recessive incomplete achromatopsia with protan luminosity function. Ophthalmologica. 1978; 177(4):197-207.
47. Wiszniewski W, Lewis RA, Lupski JR. Achromatopsia: the CNGB3 p.T383fsX mutation results from a founder effect and is responsible for the visual phenotype in the original report of uniparental disomy 14. Hum Genet. 2007; 121(3-4):433-439.
48. Talcott KE, Ratnam K, Sundquist SM, et al. Longitudinal study of cone photoreceptors during retinal degeneration and in response to ciliary neurotrophic factor treatment. Invest Ophthalmol Vis Sci. 2011; 52(5):2219-2226.

Figure Captions

Figure 1. Correlating SD-OCT and microperimetry findings from 2 patients with achromatopsia (subjects no. 2, 3). Shown are isolated patchy areas of subnormal retinal thresholds within the posterior pole compared to previously published normative data.[33]

Figure 2. High-resolution SD-OCT scans through the fovea. Scans were acquired using the Bioptigen SD-OCT and foveal location was confirmed using accompanying volume scans. Panel numbers correspond to subject numbers in **Table 1**. Note the variable appearance of the IS/OS disruption in these individuals, even in subjects with the same genotype (subjects 5, 7, 8 and subjects 6, 12). Scale bar is 1mm.

Figure 3. Images of the photoreceptor mosaic in achromatopsia. Images of the foveal cone mosaic (a) and peripheral (~10 degrees) rod and cone mosaic (b) obtained with the AOSLO for a normal subject are shown for comparison. In the peripheral image, the dark ring associated with each cone is presumably the boundary of the inner segment, while the central reflective core is from the outer segment or IS/OS junction. Note the variable appearance of the cones in the normal retina (b), with some cones being devoid of a central reflection (arrows in b). The images in panel c-e represent individual frames from the AOSLO, while f-h are from the AO flood-illuminated camera. All subjects had evidence of residual cone structure, though to a variable degree. Panel c and g are from subject 5, d is from subject 8, e is from subject 12, f is from subject 10, and h is from subject 6. Panels c-f demonstrate the presence of multiple cone inner segments that still retain a central reflective core (arrows), though it is diminished in its reflectance compared to normal. Scale bar is 50 μm.

Figure 4. Correlating SD-OCT and AOSLO findings. Shown is a section of the SD-OCT scan for subject 5, and corresponding AOSLO images from either side of the focal IS/OS disruption. The extent of this disruption (201 μm) is consistent with the reported size of the rod-free zone.[36]

Figure 5. Images of the photoreceptor mosaic at different eccentricities. All four images are from subject 12, and were taken from the central fovea (A), 2 degrees (B), 4 degrees (C), and 16 degrees (D). Retinal location was determined based on blood vessel appearance in neighboring AOSLO video frames. There is an absence of obvious cone structure in the central fovea, consistent with observations on SD-OCT. However, the number of cone inner segments increases at the 2 degree location, before falling off in the more peripheral locations. Scale bar is 100 μm.

Table 1. Summary of Structural and Functional Findings in the Study Cohort

Patient No.	Visual Acuity (log MAR)		Fundus Macular Appearance	Color Vision (anomaloscope)	Full-Field ERG			SD-OCT	AO Cone Structure	MP (dB)
					Scotopic	Photopic				
	OD	OS				single-flash b-wave amplitude	32-Hz flicker			
1	0.92	0.90	wnl (OU)	Matched (0-73)	Normal	ND	ND	Normal OS/IS in the fovea	N/A	N/A
2	0.94	0.92	blunted FR (OU)	Matched (47-73)	Normal	Severely reduced	ND	Focal OS/IS disruption (small bubble) in the fovea	Minimal cone IS structure, no visible OS reflection	OD=10.0 OS=11.3
3	0.46	0.44	blunted FR (OU)	Matched (0-73)	Normal	Severely reduced	ND	Focal OS/IS disruption in the fovea +foveal hypoplasia	Moderate cone IS structure, no visible OS reflection	OD=11.4 OS=12.2
4	0.78	0.80	blunted FR (OU)	Matched (48-73)	Mildly reduced amplitude	Severely reduced	ND	OS/IS loss and disruption (large bubble) in the fovea	Minimal cone IS structure, no visible OS reflection	N/A
5	0.94	0.90	blunted FR (OU)	Matched (0-73)	Normal	ND	ND	Focal OS/IS disruption in the fovea (small bubble) +foveal hypoplasia	Substantial cone IS structure, frequent dim OS reflection	N/A
6	0.92	0.90	wnl (OU)	Matched (35-73)	Normal	Severely reduced	ND	Normal OS/IS in the fovea	Moderate cone IS structure, no visible OS reflection	OD=11.6 OS=12.5
7	0.92	0.96	central foveal hypopigmentation with mild RPE mottling (OU)	Matched (0-73)	Normal	Severely reduced	ND	OS/IS loss (large bubble) in the fovea	No visible cone IS structure	N/A
8	0.80	0.72	atrophic macular lesion (OU)	Matched (46-73)	Normal	Severely reduced	ND	Loss and disruption of OS/IS and RPE loss and thinning in the fovea+ foveal hypoplasia	Minimal cone IS structure, no visible OS reflection	N/A
9	0.86	0.88	blunted FR (OU)	Matched (0-73)	Normal	Moderately reduced	ND	Loss and disruption of OS/IS (large bubble) in the fovea	N/A	N/A
10	0.94	0.82	hypopigmented lesions with mild RPE mottling, ,punctate drusen (OU)	Matched (49-73)	Moderately reduced amplitude	Severely reduced	ND	Focal loss and disruption of OS/IS and mild RPE thinning in the fovea + foveal hypoplasia	Minimal cone IS structure, occasional dim OS reflection	N/A
11	0.92	0.94	atrophic macular lesion (OU)	Matched (10-73)	Moderately reduced amplitude	Severely reduced	ND	Loss of OS/IS and RPE loss and thinning in the fovea + foveal hypoplasia	N/A	N/A
12	0.92	0.90	wnl (OU)	Matched (41-73)	Normal	Severely reduced	ND	Focal loss of OS/IS + foveal hypoplasia	Substantial cone IS structure, occasional dim OS reflection	OD=13.5 OS=13.2

log MAR= logarithm of minimal angle of resolution, OD=right eye, OS=left eye, OU=both eyes, wnl=within normal limits, FR=foveal reflex, OS/IS= outer segment/inner segment junction of the photoreceptors, RPE= retinal pigment epithelium, ND= non-detectable, SD-OCT=spectral-domain optical coherence tomography, AO=adaptive optics, MP=microperimetry, N/A= not available.

Table 2. Summary of Genetic Mutations Screening Results in the Study Cohort

Patient No.	Age (yrs)/ Sex	Race/Ethnicity	Gene	Allele 1	Allele 2
1	13/F	Hispanic	No mutations found		
2	15/M	Caucasian	*CNGA3* exons 6 and 7, heterozygous	c.661C>T - Arg221Stop, exon 6	c.830G>A - Arg277His, exon 7
3	30/F	Caucasian	*CNGB3* exon10, heterozygous	c.1148delC - Thr383 del1aC	Not found
4	50/M	Lebanese	*CNGA3* exon 7, homozygous	c.1709G>T- Ser570Ile	c.1709G>T- Ser570Ile
5	15/M	Caucasian	*CNGB3* exon 10, homozygous	c.1148delC - Thr383 del1aC	c.1148delC - Thr383 del1aC
6	17/F	Jordanian	*CNGA3* exon7, heterozygous	c.985G>T - Gly329Cys	c.1306C>T - Arg436Trp
7	27/F	Caucasian	*CNGB3* exon 10, homozygous	c.1148delC - Thr383 del1aC	c.1148delC - Thr383 del1aC
8	49/M	Caucasian	*CNGB3* exon 10, homozygous	c.1148delC - Thr383 del1aC	c.1148delC - Thr383 del1aC
9	33/M	Hispanic	*CNGA3* exon 7, heterozygous	c.1228C>T - Arg410Trp	c.1541A>T - Asp514Val
10	55/M	Caucasian	*CNGB3* exon 10, heterozygous	c.1148delC - Thr383 del1aC	Not found
11	52/F	African American	*CNGA*3 exon 7, heterozygous	c.848G>A - Arg283Gln	c.1306C>T - Arg436Trp
12	14/M	Jordanian	*CNGA3* exon7, heterozygous	c.985G>T - Gly329Cys	c.1306C>T - Arg436Trp

M=Male; F=Female.

DNA numbering is based on cDNA sequence (GenBank: AF065314.1); nucleotide +1 is the A of the start codon (ATG).

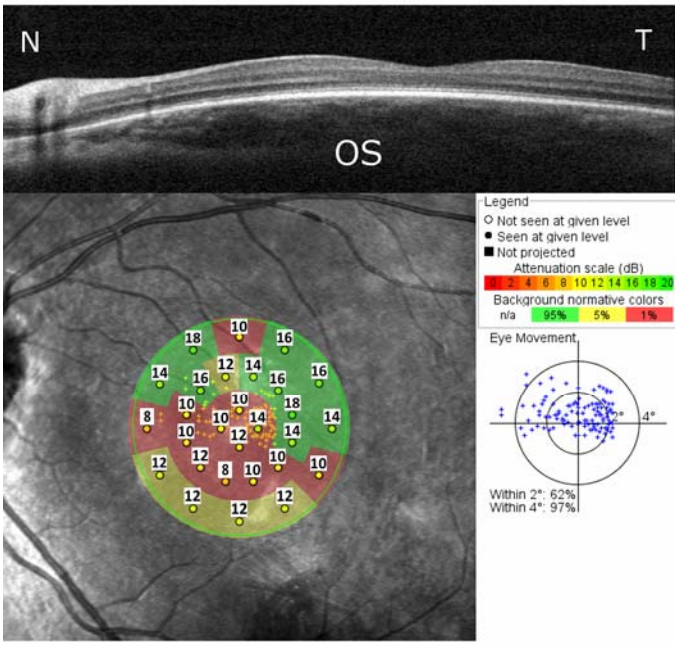
N
T
OS
Legend
Not seen at given level
Seen at given level
Not projected
Attenuation scale (dB)
0 2 4 6 8 10 12 14 16 18 20
Background normative colors
n/a 95% 5% 1%
Eye Movement
2°
4°
Within 2°: 62%
Within 4°: 97%

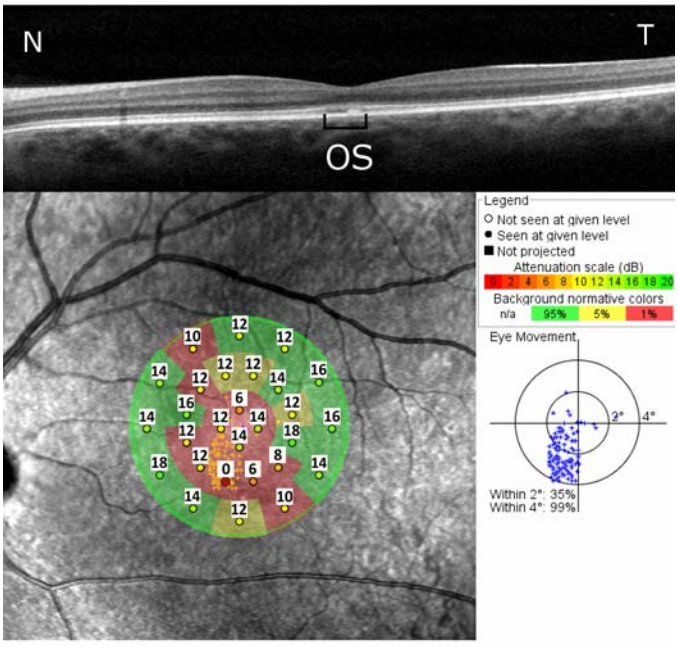
N
T
OS
Legend
Not seen at given level
Seen at given level
Not projected
Attenuation scale (dB)
0 2 4 6 8 10 12 14 16 18 20
Background normative colors
n/a 95% 5% 1%
Eye Movement
2°
4°
Within 2°: 35%
Within 4°: 99%

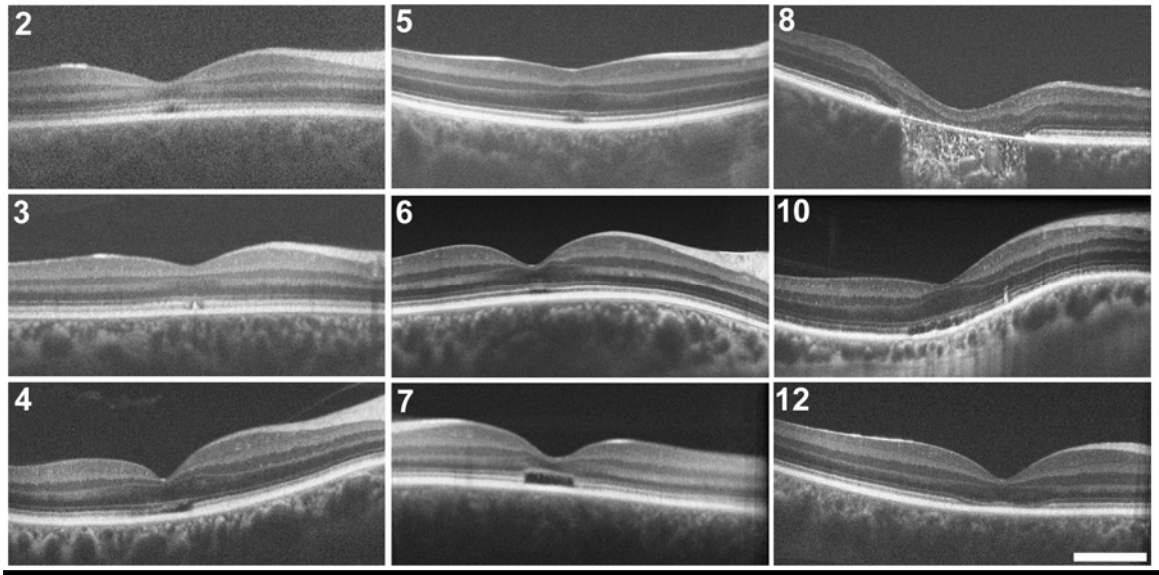
2
5
8
3
6
10
4
7
12

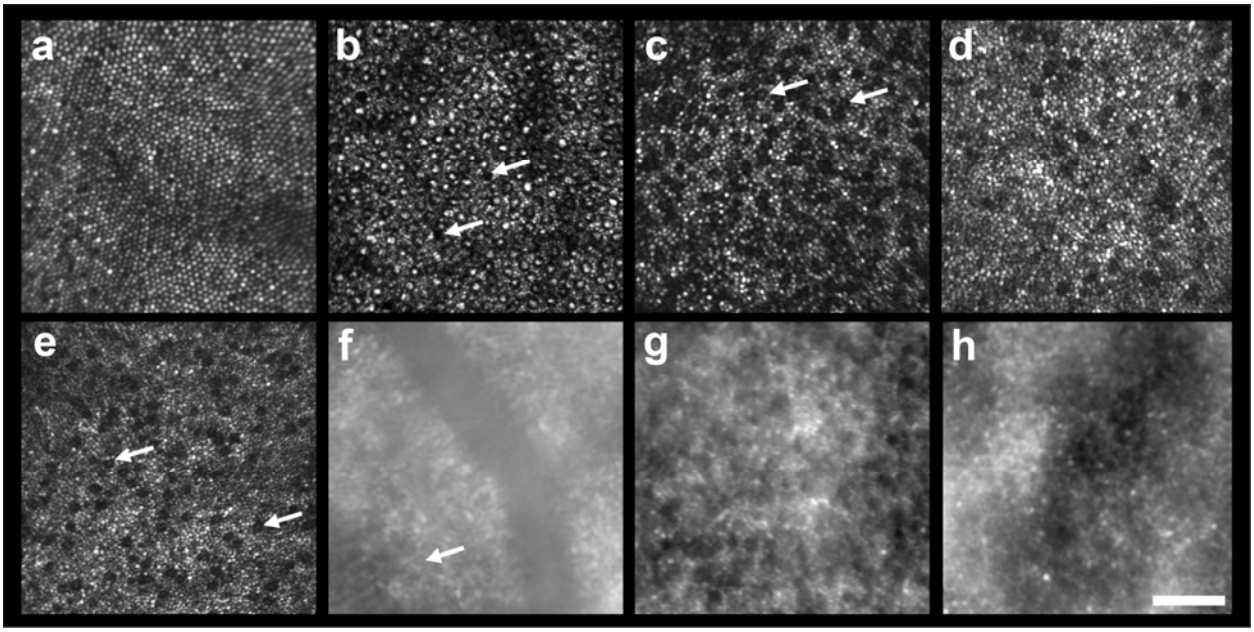
a
b
c
d
e
f
g
h

Genead et al